A New Approach to Calculate the Piezoelectric Coefficient of Piezo-Semiconductor Nanowires Integrated in Nanocomposites: Experiment and Simulation

Andres Jenaro Lopez Garcia, Ran Tao, Mireille Mouis, Gustavo Ardila

Author version. Original paper published by IEEEE Conference Proceedings (Transducers 2021), pages 1056-1059, doi:10.1109/TRANSDUCERS50396.2021.9495621

A NEW APPROACH TO CALCULATE THE PIEZOELECTRIC COEFFICIENT OF PIEZO-SEMICONDUCTOR NANOWIRES INTEGRATED IN NANOCOMPOSITES: EXPERIMENT AND SIMULATION

Andrés Jenaro Lopez Garcia[1], Ran Tao[2], Mireille Mouis[1] and Gustavo Ardila[1]
[1] University Grenoble Alpes, Univ. Savoie Mont Blanc, CNRS, Grenoble INP, IMEP-LaHC, Grenoble, FRANCE and [2]Key Laboratory of Optoelectronic Devices and Systems of Ministry of Education and Guangdong Province, College of Physics and Optoelectronic Engineering, Shenzhen University, Shenzhen 518060, CHINA.

ABSTRACT
Piezoelectric semiconductor transducers based on nanowires (NWs) made of ZnO, GaN among other materials have drawn a lot of attention for energy harvesting and sensing applications. Despite the existence of experimental reports on the piezoelectric coefficient d_{33} of ZnO NWs using Piezoelectric Force Microscopy (PFM), there is a lack of theoretical results predicting such measurements. Here we propose an experimental and a simulation framework consisting in the analysis of the exponential decay of a generated piezoelectric voltage pulse to extract the capacitance of ZnO NW based nanocomposites and the related d_{33}. The theoretical results show a d_{33} dependency on the NW radius, thus achieving high values (14 pC/N) at radius smaller than 70 nm.

KEYWORDS
Piezoelectricity, semiconductor, surface traps, ZnO.

INTRODUCTION
Piezoelectric transducers integrating nanowires (also known as NanoGenerators - NGs) have been widely studied in the last decade as energy sources for self-powered systems such as wireless sensors [1]. In particular, NG based on piezo-semiconductor nanowires (NWs), such as ZnO [2], GaN [3] among others, have been used for developing energy harvesting devices and mechanical sensors. ZnO NWs have been used as active material due to its good piezoelectric properties compared to its bulk counterpart, an because its ease of manufacturing at low temperatures using Chemical Bath Deposition (CBD) [4]. Some experiments have demonstrated that NGs can generate a relatively high output potential [5]–[7] whereas reported theoretical reports could not explain this good performance due to the screening effect of free electrons that reduced the output potential [8]–[11]. A recent theoretical approach using Surface Fermi Level Pinning (SFLP) in ZnO NWs was proposed to clarify this contradiction [12]. Although up to now, the calculation of d_{33} has not been explored considering the piezoelectric and semiconductor coupling, this can open the possibility of exploring the figure of merits of the related devices (i.e. sensitivity, efficiency, etc.) [13].

In this work, we present an experimental and theoretical framework to calculate the d_{33} coefficient of piezoelectric semiconducting NWs integrated in composites and evaluated under a controlled compressive force. We analyze the exponential decay of the piezoelectric generated signals which provide useful information about the internal capacitance of the nanocomposite (i.e., capacitance of the NG) allowing the calculation of the d_{33} coefficient.

FABRICATION OF THE ZNO NANOCOMPOSITE AND THEORETICAL FRAMEWORK:
A ZnO seed layer was deposited on a Si substrate by Atomic Layer Deposition (ALD) at 250°C. Then, CBD was carried out to grow ZnO NWs. Spin coating was used to encapsulate the NWs with a polymer matrix made of poly(methyl methacrylate) (PMMA) as previously reported [14].

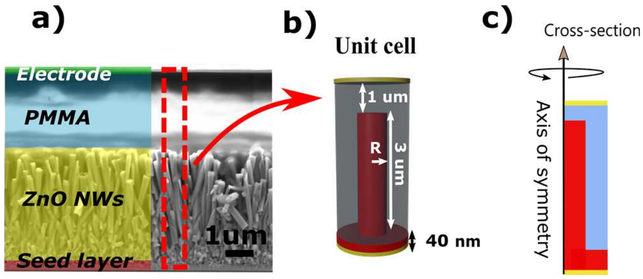

Fig. 1: a) SEM cross section of a nanocomposite (NanoGenerator) integrating vertical ZnO NWs arrays. b) Unit cell model of a ZnO based NG and c) 2D-axisymmetric model built in COMSOL software.

According to the SEM (Scanning Electron Microscopy) image of the device cross-section (see Fig. 1a), the ZnO seed layer thickness is about 40nm. The dimension of the ZnO NW is in the range of 80-120 nm in radius and 3 µm in length. Additionally, the top layer of the PMMA matrix above the ZnO surface is about 1 µm. Once the real parameters of the ZnO device are known, a model of the structure was built using the Finite Element Method (FEM) under the COMSOL software environment as shown in Fig. 1b. A unit cell of the whole structure is made with specific boundary conditions to represent the behavior of the whole device [15]. The unit cell is further simplified using a 2D-axisymmetric structure to reduce computational cost (see Fig. 1c). Piezoelectric and semiconductor coupling was considered in this study including free carriers and surface traps inducing the surface Fermi level pinning [12].

Author version. Original paper published by IEEEE Conference Proceedings (Transducers 2021), pages 1056-1059, doi:10.1109/TRANSDUCERS50396.2021.9495621

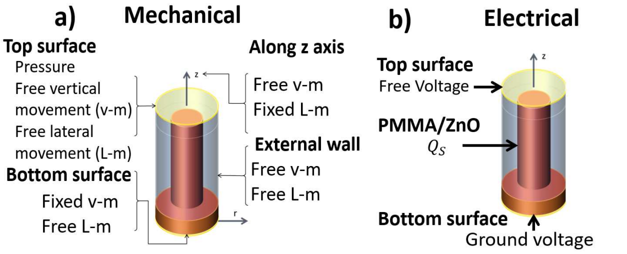

Fig. 2: a) Mechanical and b) electrical boundary conditions used in COMSOL software.

Fig. 2a schematizes the mechanical boundary conditions. A vertical compressive force is applied on the top surface of the unit cell and a fixed constraint is established at the bottom along the z-direction. Fig. 2b shows the electrical boundary conditions. The electrical ground is placed at the bottom. An electric surface charge (Q_s) is placed on the entire surface of ZnO, which in turn is a function of the local potential (V) and the surface traps density (N_{it}) [12]. To analyze rigorously the output potential and other electrical parameters in compressive mode, we have calculated the difference of all those quantities for a system without applied force (called initial state) and a system with applied force (called final state). The input parameters used in this model were taken from the electromechanical experiment as described in the next section. The doping level and surface trap density values were taken from the literature related to the growing technique of ZnO NWs (CBD) as shown in Table1.

Table 1: Input parameters used in the simulation.

Input parameter	Value
Pressure (kPa)	50-100
Doping level (cm^{-3})	$5 \cdot 10^{17}$ [16]
Trap density ($eV^{-1}cm^{-2}$)	10^{13} [17]

EXPERIMENTAL RESULTS

Figure 3a show the electromechanical test-bench used to apply a controlled compressive force. This system is composed of an actuator, a sample holder, a load force, and a force sensor. The ZnO NG is placed between the sample holder and a ceramic rod, used to apply pressure on the piezo sample. This force is controlled thanks to the force sensor that is connected to the ceramic rod. Then, the electrodes of the ZnO NG are attached to a voltage amplifier with a load input resistance (R_L) of 100 MΩ.

As shown in Fig. 3b, when a compressive force of ~5N (about 50kPa) is applied to the sample, a voltage of 80 mV is generated between its electrodes. This voltage is a product of the polarization field inside the NG and it is able to move electrons from the external circuit (i.e. an electric current) to compensate the voltage drop. An exponential decay of the voltage is evidenced as it happens in a discharging capacitor (see Fig. 3b). To extract the capacitance from the NG, the voltage in function of time is plotted in a logarithmic scale (see inset of Fig. 3b) and the slope of the linear fit is calculated. By considering the NG as a capacitor discharging over a resistive load, the equation (Eq.1) can be used to calculate the NG capacitance ($\bar{C}_0'$). In this case $\bar{C}_0'$ is equal to 300 pF.

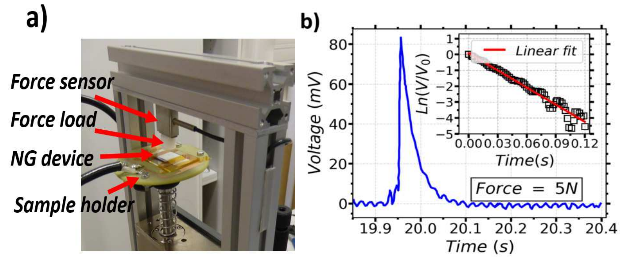

Fig. 3: a) Electromechanical test-bench b) generated voltage signal under a compressive force. The inset figure is the logarithm of the voltage as a function of time.

$$Log\frac{V(t)}{V_0} = -\frac{t}{R_{load}\bar{C}_0'} \quad (1)$$

To calculate the d_{33} of the ZnO NWs on this device, we used Eq.2 as a function of the generated voltage, the applied force, and the capacitance.

$$d_{33} = \frac{\bar{C}_0' * V}{F_{applied}} \quad (2)$$

Replacing all those quantities and assuming that all the compressive pressure is along the z-direction, the calculated d_{33} is about 4.8 pC/N.

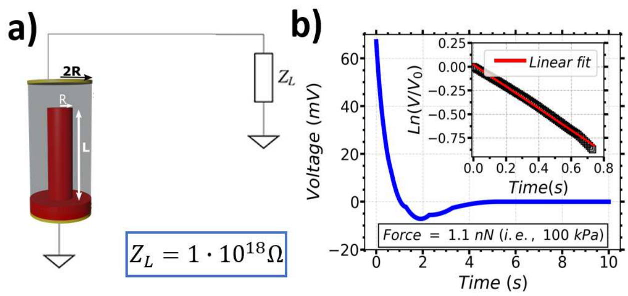

Fig. 4: a) Schematic of the ZnO NG cell model connected to a resistive load and b) absolute value of the generated voltage signal after applying a compressive force. The inset figure is the logarithm of the voltage as a function of time.

SIMULATION RESULTS

Capacitance calculation:

In order to calculate the capacitance of the NG unit cell (C_{NG}), a time-dependent study is performed by connecting a resistive load (Z_L) to the NG cell as shown in Fig. 4a. Fig. 4b shows an example of such simulation considering a ZnO NW 3µm long and 60nm in radius. A constant force of 1.1 nN (i.e., 100 kPa of pressure) is applied on the top surface of the unit cell generating a voltage which decays exponentially in function of time. A high Z_L value ($1\,x\,10^{18}\,\Omega$) was used to avoid the internal resistance contribution in this pulse decay. A high internal resistance is expected because of the small dimensions of the NG cell compared to the complete device. Using the same procedure to extract the capacitance, as described in the precedent section, allow us to extract a C_{NG} value of

Author version. Original paper published by IEEEE Conference Proceedings (Transducers 2021), pages 1056-1059, doi:10.1109/TRANSDUCERS50396.2021.9495621

$8.69\,x\,10^{-19}\,F$ which is comparable with reported simulation works on this same scale [18], [19]. This value is not comparable with the experimental one because the cell surface area is much smaller than the whole device, but it is useful to calculate the d_{33} value as shown below.

d_{33} as a function of the ZnO NW radius:

The model allows the calculation of d_{33} in function of different parameters. A sweeping was made of all variables involved in Eq. 2 as a function of the NW radius for two values of applied pressure: 50 and 100kPa. Fig.5a. shows the maximum voltage calculated (at t=0) as a function of the ZnO NW radius. At low radii values, a compressive pressure of 100 kPa can generate a voltage (~68 mV) about 2 times higher than at a presure of 50kPa (~34 mV). At higher values of radius (> 60 nm), the voltage values in both cases are considerably reduced to a few millivolts due to a strong screening effect generated by free charges [8]–[11]. The piezopotential obtained in the experiment (~80mV at about 50kPa) is within the same order of magnitude as the one obtained in the simulation (34-68 mV for a pressure between 50-100 kPa), although for NW radius relatively smaller (<70nm) compared to those present in the actual device (80-120nm). This can be explained because in the experiment, not all the NWs have the same size, they are not all vertically oriented [20] and the semiconducting properties (N_{it} and N_d) could differ from the considered values from the literature.

Fig. 5b shows the increasing of the capacitance value of the NG cell as the ZnO NW radius is increased, this is expected considering the relationship between capacitance and area (i.e. $C \propto A$).

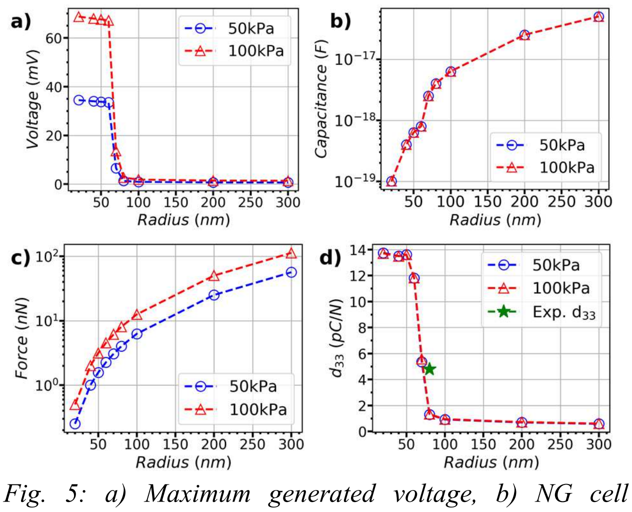

Fig. 5: a) Maximum generated voltage, b) NG cell capacitance, c) corresponding applied force on the NG cell and d) d_{33} values as a function of the NW radius for two values of applied pressure.

According to the Eq.2 and at first glance, we could expect that the d_{33} would increase if the voltage is increased by changing the applied pressure. But d_{33} is an intrinsic property and it must be a quantity independent of both the applied pressure and the generated voltage. Fig. 5a. and Fig. 5c. show that there is actually a compensation between the high voltage values produced at high pressures and the lower voltage values at low pressures through the applied force. Combining all the calculated values and using Eq.2, we can determinate the d_{33} value as a function of the ZnO NW radii. Fig. 5d. shows that d_{33} have a maximum value of about 14pC/N at low NW radius and is decreased up to a value of 1pC/N at high radius. There is thus a radius dependency of d_{33} which is related to the distribution of free charges by the presence of a surface traps density [12]. Nevertheless, it confirms that there is not any dependency of the d_{33} value with the applied pressure or with the generated voltage.

It should be noted that the calculated d_{33} values are within the range of experimental [21], [22] and theoretically reports [23] (i.e., between 2-12 pC/N). Moreover, the experimental value determined in this work (as it is pointed out by the green star in Fig.5d) is also within this range of values for a ZnO NW with radius close to 70 nm. It is also important to mention that in the absence of semiconducting properties, such models would result in a constant value of d_{33} for the radius range evaluated in this work [24].

CONCLUSIONS

This work shows an alternative method to calculate the d_{33} coefficient of piezoelectric semiconducting NWs, which is a fundamental parameter to estimate the efficiency of related piezoelectric transducers. It consists in applying a controlled compressive force on a composite integrating vertically oriented NWs and analyzing the exponential decay of the generated voltage pulse. The experimental d_{33} value of ZnO NWs 3µm long and with diameter between 80-120nm is close to 4.8 pC/N. The simulation results considering semiconductor properties and in particular surface traps are coherent with the experimental results for NWs with radius close to 70nm. Additionally, our simulations show that the d_{33} does not depend on the applied pressure and on the generated voltage as expected. However, there is a radius dependency of d_{33}, reaching a maximum value of about 14 pC/N for radius smaller than 70 nm. Whereas for larger radius d_{33} tends to 1 pC/N. Our results are also in good agreement with the d_{33} values reported in the literature (between 2-12 pC/N). Our models suggest that this radius dependency is due to semiconductor properties such as doping level and surface trap density.

REFERENCES

[1] A. Nechibvute, A. Chawanda, P. Luhanga, and A. R. Akande, "Piezoelectric energy harvesting using synchronized switching techniques," *Int. J. Eng. Technol.*, vol. 2, no. 6, pp. 936–946, 2012.

[2] M.-H. Zhao, Z.-L. Wang, and S. X. Mao, "Piezoelectric Characterization of Individual Zinc Oxide Nanobelt Probed by Piezoresponse Force Microscope," *Nano Lett.*, vol. 4, no. 4, pp. 587–590, Apr. 2004.

[3] C.-H. Wang *et al.*, "Optimization of the Output Efficiency of GaN Nanowire Piezoelectric Nanogenerators by Tuning the Free Carrier

Author version. Original paper published by IEEEE Conference Proceedings (Transducers 2021), pages 1056-1059, doi:10.1109/TRANSDUCERS50396.2021.9495621

Concentration," *Adv. Energy Mater.*, vol. 4, no. 16, p. 1400392, Nov. 2014.

[4] F. D. Nayeri, E. A. Soleimani, and F. Salehi, "Synthesis and characterization of ZnO nanowires grown on different seed layers: the application for dye-sensitized solar cells," *Renew. Energy*, vol. 60, pp. 246–255, 2013.

[5] S. Xu, Y. Qin, C. Xu, Y. Wei, R. Yang, and Z. L. Wang, "Self-powered nanowire devices," *Nat. Nanotechnol.*, vol. 5, no. 5, p. 366, 2010.

[6] Y. Hu, L. Lin, Y. Zhang, and Z. L. Wang, "Replacing a battery by a nanogenerator with 20 V output," *Adv. Mater.*, vol. 24, no. 1, pp. 110–114, 2012.

[7] G. Zhu, A. C. Wang, Y. Liu, Y. Zhou, and Z. L. Wang, "Functional electrical stimulation by nanogenerator with 58 v output voltage," *Nano Lett.*, vol. 12, no. 6, pp. 3086–3090, 2012.

[8] R. Araneo, G. Lovat, P. Burghignoli, and C. Falconi, "Piezo-semiconductive quasi-1D nanodevices with or without anti-symmetry," *Adv. Mater.*, vol. 24, no. 34, pp. 4719–4724, 2012.

[9] Y. Gao and Z. L. Wang, "Equilibrium potential of free charge carriers in a bent piezoelectric semiconductive nanowire," *Nano Lett.*, vol. 9, no. 3, pp. 1103–1110, 2009.

[10] G. Romano, G. Mantini, A. Di Carlo, A. D'Amico, C. Falconi, and Z. L. Wang, "Piezoelectric potential in vertically aligned nanowires for high output nanogenerators," *Nanotechnology*, vol. 22, no. 46, p. 465401, Nov. 2011.

[11] G. Mantini, Y. Gao, A. D'amico, C. Falconi, and Z. L. Wang, "Equilibrium piezoelectric potential distribution in a deformed ZnO nanowire," *Nano Res.*, vol. 2, no. 8, pp. 624–629, 2009.

[12] R. Tao, M. Mouis, and G. Ardila, "Unveiling the Influence of Surface Fermi Level Pinning on the Piezoelectric Response of Semiconducting Nanowires," *Adv. Electron. Mater.*, vol. 4, no. 1, pp. 1–9, 2018.

[13] J. I. Roscow, H. Pearce, H. Khanbareh, S. Kar-Narayan, and C. R. Bowen, "Modified energy harvesting figures of merit for stress-and strain-driven piezoelectric systems," *Eur. Phys. J. Spec. Top.*, vol. 228, no. 7, pp. 1537–1554, 2019.

[14] R. Tao *et al.*, "Performance of ZnO based piezo-generators under controlled compression," *Semicond. Sci. Technol.*, vol. 32, no. 6, 2017.

[15] R. Hinchet, S. Lee, G. Ardila, L. Montès, M. Mouis, and Z. L. Wang, "Performance optimization of vertical nanowire-based piezoelectric nanogenerators," *Adv. Funct. Mater.*, vol. 24, no. 7, pp. 971–977, 2014.

[16] T. Cossuet, F. Donatini, A. M. Lord, E. Appert, J. Pernot, and V. Consonni, "Polarity-Dependent High Electrical Conductivity of ZnO Nanorods and Its Relation to Hydrogen," *J. Phys. Chem. C*, vol. 122, no. 39, pp. 22767–22775, Oct. 2018.

[17] Q. Zhao, L.-L. Yang, B. Sernelius, P.-O. Holtz, and M. Willander, "Surface recombination in ZnO nanorods grown by chemical bath deposition," *J. Appl. Phys.*, vol. 104, no. 7, p. 73526, 2008.

[18] N. Doumit and G. Poulin-Vittrant, "Effect of the Dielectric and Mechanical Properties of the Polymer Matrix on ZnO-Nanowire-Based Composite Nanogenerators Performance," *Adv. Theory Simulations*, vol. 3, no. 9, p. 2000128, 2020.

[19] N. Doumit and G. Poulin-Vittrant, "A new simulation approach for performance prediction of vertically integrated nanogenerators," *Adv. Theory Simulations*, vol. 1, no. 6, p. 1800033, 2018.

[20] G. Ardila, R. Tao, R. Hinchet, L. Montès, and M. Mouis, "Will composite nano-materials replace piezoelectric thin films for energy transduction?," in *2015 Advanced Research Workshop Future Trends in Microelectronics: Journey into the Unknown*, 2015.

[21] E. Broitman, M. Y. Soomro, J. Lu, M. Willander, and L. Hultman, "Nanoscale piezoelectric response of ZnO nanowires measured using a nanoindentation technique," *Phys. Chem. Chem. Phys.*, vol. 15, no. 26, pp. 11113–11118, 2013.

[22] D. Tamvakos *et al.*, "Piezoelectric properties of template-free electrochemically grown ZnO nanorod arrays," *Appl. Surf. Sci.*, vol. 356, pp. 1214–1220, Nov. 2015.

[23] M. Catti, Y. Noel, and R. Dovesi, "Full piezoelectric tensors of wurtzite and zinc blende ZnO and ZnS by first-principles calculations," *J. Phys. Chem. Solids*, vol. 64, no. 11, pp. 2183–2190, Nov. 2003.

[24] S. M. Kim *et al.*, "Radially dependent effective piezoelectric coefficient and enhanced piezoelectric potential due to geometrical stress confinement in ZnO nanowires/nanotubes," *Appl. Phys. Lett.*, vol. 101, no. 1, p. 013104, Jul. 2012.

ACKNOWLEDGEMENTS

This work was supported by the Federation of Micro Nano Technologies (FMNT) in Grenoble, France and has received funding from project PULSE-COM of the European Union's Horizon 2020 research and innovation programme under grant agreement No 863227. The authors further acknowledge the support from the CNRS Renatech Network through the "Plateforme Technologique Amont" in a cleanroom environment.

CONTACT

*A.J. López, tel: +33-6-35362308; andres-jenaro.lopez-garcia@grenoble-inp.fr